

Controlled Growth of Cu_{2-x}S Sheet-like Nanoshells and Cu_{2-x}S -CdS p-n Junctions on Au Nanorods with Coupled Plasmon Resonances and Enhanced Photocatalytic Activities

Wei Wang,^{‡a} Song Ma,^{‡a} Kai Chen,^{‡b} Peng-Fei Wang,^a Qi-Yu Liu,^a Li Zhou^{*a} and Qu-Quan Wang^{*a,b}

^aKey Laboratory of Artificial Micro- and Nano-structures of the Ministry of Education, School of Physics and Technology, Wuhan University, Wuhan 430072, P. R. China.

^bThe Institute for Advanced Studies, Wuhan University, Wuhan 430072, P. R. China.

*Email: qqwang@whu.edu.cn (Qu-Quan Wang), zhouli@whu.edu.cn (Li Zhou).

[‡]These authors equally contributed to this work.

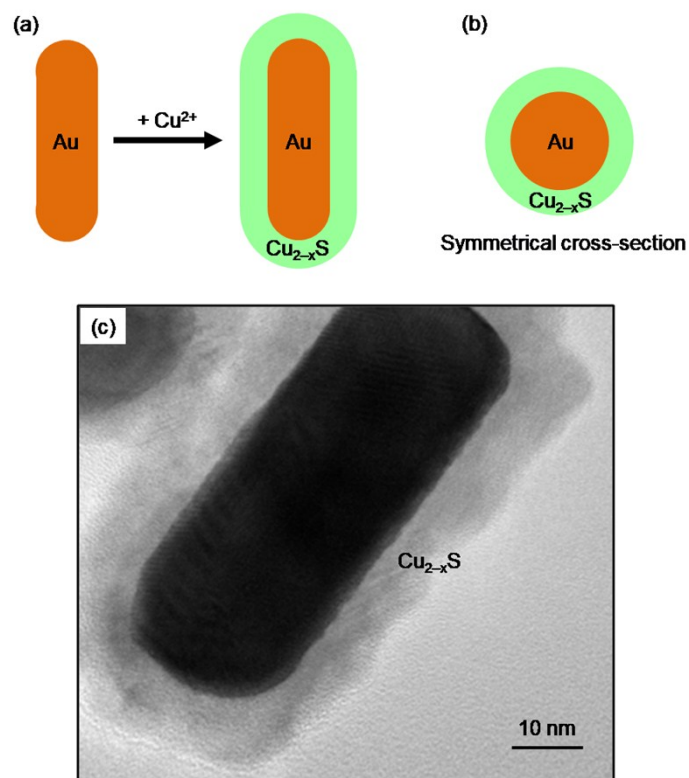


Figure S1 Structural diagram and TEM image of the general Au/Cu_{2-x}S core-shell heterorods with symmetric vertical cross-section. (a) The schematic diagram of uniformly growing the Cu_{2-x}S shells on Au nanorods. (b) The symmetric cross-section of Au/Cu_{2-x}S core-shell nanorods. (c) TEM image of Au/Cu_{2-x}S nanorods with uniform Cu_{2-x}S shells.

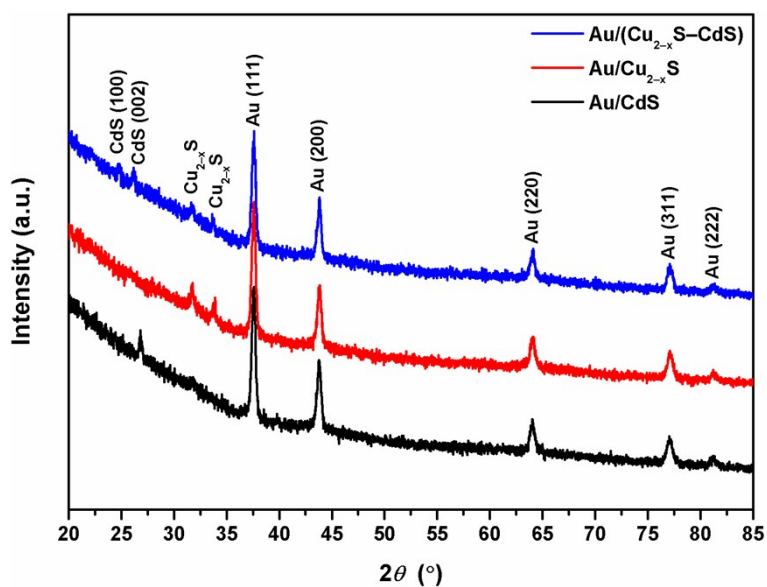


Figure S2 XRD patterns of the three core-shell heterorods of Au/CdS ($\mu_{\text{Cd}} = 20 \mu\text{L}$), Au/Cu_{2-x}S ($\mu_{\text{Cu}} = 20 \mu\text{L}$) and Au/(Cu_{2-x}S-CdS) ($\mu_{\text{Cu}} = 20 \mu\text{L}$, $\mu_{\text{Cd}} = 20 \mu\text{L}$).

Table S1 The atomic concentration of each constituent element in Au/(CdS–Ag₂S) ($\mu_{\text{Cd}} = 20 \mu\text{L}$, $\mu_{\text{Ag}} = 15 \mu\text{L}$), Au/(Cu_{2-x}S–Ag₂S) ($\mu_{\text{Cu}} = 20 \mu\text{L}$, $\mu_{\text{Ag}} = 15 \mu\text{L}$) and Au/(Cu_{2-x}S–CdS) core-shell heterorods ($\mu_{\text{Cu}} = 20 \mu\text{L}$, $\mu_{\text{Cd}} = 20 \mu\text{L}$).

	S 2p (%)	Cd 3d (%)	Cu 2p (%)	Au 4f (%)	Ag 3d (%)	Other elements (%)
Au/(Cu _{2-x} S–CdS)	14.53	5.58	3.67	7.68	2.71	65.84
Au/(Cu _{2-x} S–Ag ₂ S)	11.47	---	4.96	7.98	5.63	69.96
Au/(CdS–Ag ₂ S)	12.26	5.18	---	7.44	5.17	69.95

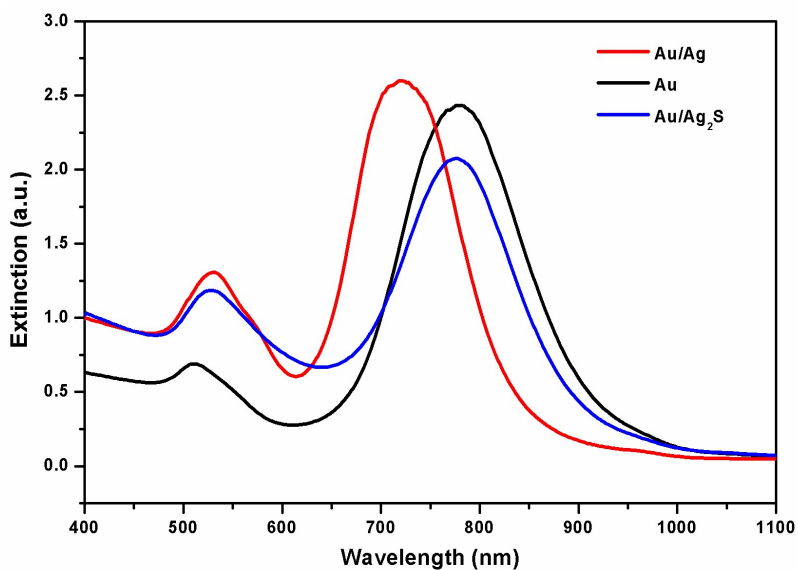


Figure S3 Extinction spectra of Au, Au/Ag, and Au/Ag₂S nanorods used in the growth process of Cu_{2-x}S nanosheets and Cu_{2-x}S–CdS p-n heterojunctions on Au nanorods.

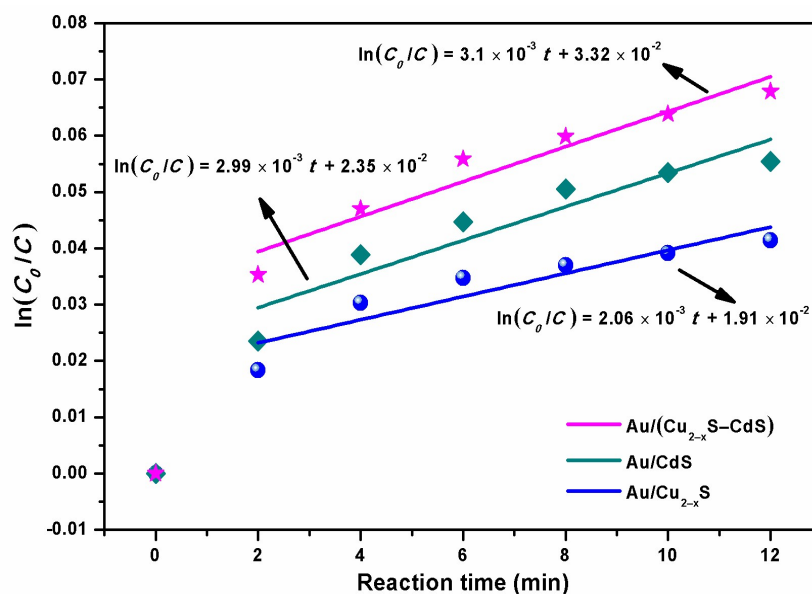


Figure S4 Kinetics fitting of $\ln(C_0/C)$ versus time (t) for the degradation of RhB by $\text{Au}/(\text{Cu}_{2-x}\text{S}-\text{CdS})$, Au/CdS and $\text{Au}/\text{Cu}_{2-x}\text{S}$ photocatalysts.

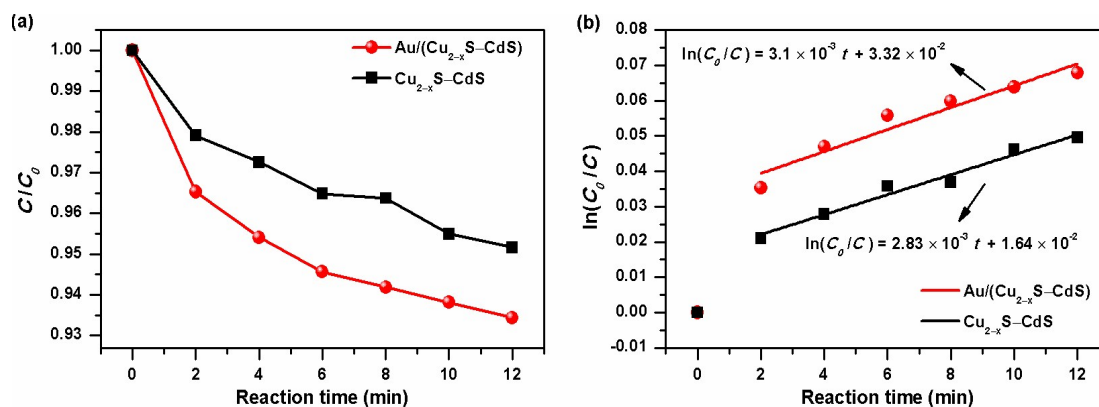


Figure S5 Comparison of photocatalytic performances between $\text{Au}/(\text{Cu}_{2-x}\text{S}-\text{CdS})$ heterorods and $\text{Cu}_{2-x}\text{S}-\text{CdS}$ p-n junctions ($\mu_{\text{Cu}} = 20 \mu\text{L}$, $\mu_{\text{Cd}} = 25 \mu\text{L}$). (a) Photocatalytic degradation curve. (b) Kinetics fitting of $\ln(C_0/C)$ versus time (t) for the degradation of RhB. The measurement method of photocatalytic activity of $\text{Cu}_{2-x}\text{S}-\text{CdS}$ p-n junctions without Au component is the same as that of photocatalytic reactions of $\text{Au}/(\text{Cu}_{2-x}\text{S}-\text{CdS})$.

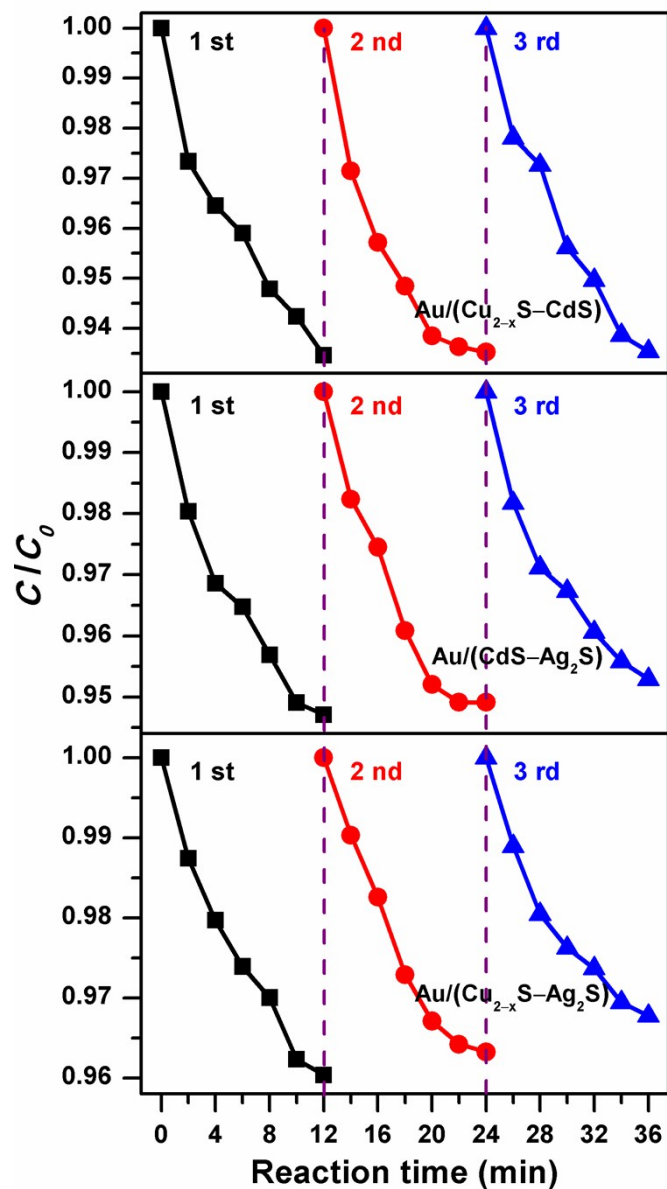


Figure S6 The recycling test for the photodegradation of RhB by the $Au/(Cu_{2-x}S-CdS)$, $Au/(Cu_{2-x}S-Ag_2S)$ and $Au/(CdS-Ag_2S)$ heterorods under visible light irradiation ($\lambda > 420$ nm). The recycling test of the photocatalysts is performed under the same conditions as the photocatalytic test.

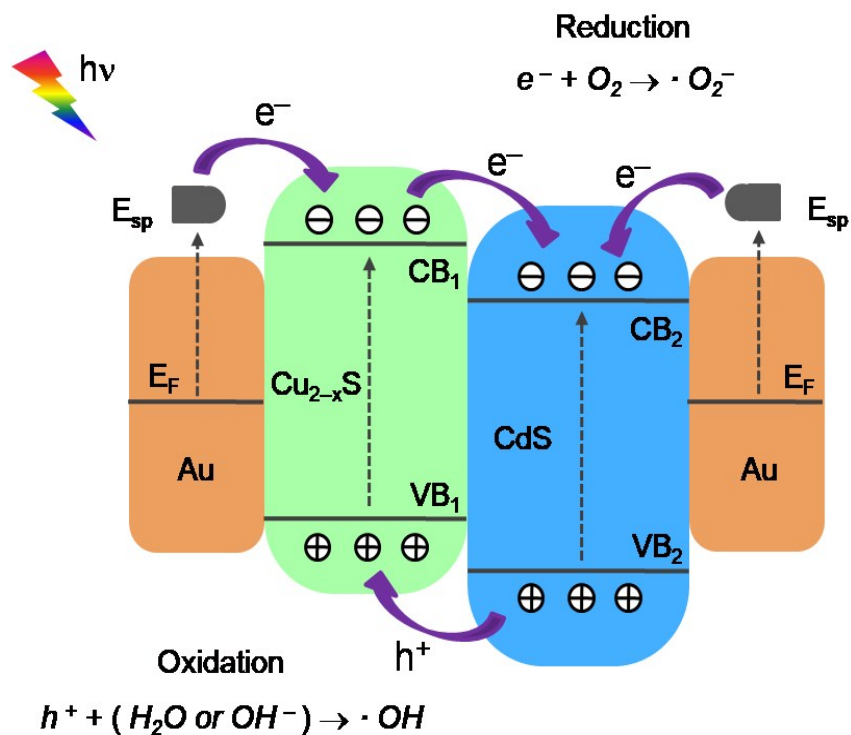


Figure S7 The possible charge transfer mechanism involved in the process of photodegradation of RhB by the Au/(Cu_{2-x}S–CdS) core-shell heterorods. $h\nu$, photon energy; e^- , electron; h^+ , hole; CB, conduction band; VB, valence band; $\cdot OH$, hydroxyl radical; $\cdot O_2^-$, superoxide radical; E_F , Au Fermi level; E_{sp} , Au surface plasmon state.